PATHOS DELIVERABLE D2.5: NON-MARKOVIAN PROBES

Report on the environment characterisation via non-Markovian probes

The interaction between a physical system and the external environment can lead to non-Markovian (memory) effects, i.e. the influence of the environment on the system depends on the past history of the system dynamics [1, 2]. In the context of sensing as in PATHOS, one has to take into account the system/sample to be investigated and the system used as probe. At the mesoscopic scale, the dimension of the probe is usually smaller than the dimension of the measured sample, which for the probe has to be considered in all respects as an environment with many degrees of freedom. Thus, it is common to assume that the interaction (in the sense of dynamical coupling) between the sample and the probe induces perceptible effects only on the probe and leaves practically unchanged the main features of the sample. In this way, the observation of the interaction effects on the probe dynamics allows to extract information on the sample. The goal is to characterize the sample with the largest possible accuracy. The latter strictly depends on the way the probe interacts with the sample, and in particular on sensitive parameters such as the distance between them and/or the initial state/energy of the probe before the interaction stage. This consideration tells us that there exists a correlation between the phenomena governing the sample-probe interaction and the sensitivity that can be achieved for the inference of specific features of the sample.

In this report we mainly focus on several non-Markovian effects induced on the selected quantum probe by the interaction with the sample. In particular, below we will specifically discuss the following three main aspects:

1. Characterize non-Markovian behaviours of a quantum probe, specifically in relation with time-monitoring schemes and multi-time statistics.

2. Extract information on specific features of the sample, by measuring non-Markovian effects in the probe (induced by the interaction with the sample).

3. Evaluate if the extracted information on the sample is complete or sufficiently accurate, and understand how this depends on whether the sample-probe interaction induces Markovian or non-Markovian phenomena on the probe itself.

These aspects are currently tested by using optical platforms and nitrogen-vacancy (NV) center experimental systems, as described in the following sections.

I. Characterization of non-Markovianity via multi-time statistics (UNIFI)

Firstly, we have provided a new characterization of these memory effects originated by the interaction between a quantum system $\mathbb{S}$ and an external environment $\mathbb{E}$. As explained above, $\mathbb{S}$ and $\mathbb{E}$ could be seen as the probe and the sample to be investigated, respectively. By the formalism of open quantum systems, we have assumed that the system and the environment are modelled as a composite system with unitary dynamics, thus governed by a purely Hamiltonian evolution. Being our study finalized to sensing purposes, we have specifically studied the possibility to monitor the formation of non-Markovian behaviours within $\mathbb{S}$ by applying a sequence of quantum measurements on the quantum system [3]. Thus, to each measurement corresponds a probabilistic outcome that depends not only on the system but also on the specific interaction with the environment. More formally, we say that such information on the environment is encoded in the so-called "multi-time statistics" that is expressed as a function of the stochastic dynamics of the system conditioned to the occurrence of the measurement operators. *We have identified in the multi-time statistics the adequate key quantity to be considered to infer features of* $\mathbb{E}$.

The effects on the system dynamics given by applying sequences of quantum measurements (at properly chosen time instants) give rise to purely quantum features, which cannot be retrieved by any classical transformations. In particular, any measurement procedure is defined by n distinct time instants $t_{\rm fin} \equiv t_m > t_{m-1} > \ldots > t_1 > t_0 \equiv 0$ (not necessarily equi-distributed in time) within the range of time $[0, t_{\rm fin}]$, and consists in locally applying a sequence of measurements, each of them in correspondence of such time instants t_k, $k = 1, \ldots, m$. Here, a subtle point emerges: from one hand the non-Markovianity of a system dynamics depends on its interaction with the environment and the only way to probe it is by performing sequential measurements. On the other hand, any set of sequential measurements modifies the system dynamics, and then also the memory effects within its dynamics. It appears clear that these two phenomena (the interaction with the environment and the monitoring of an external observer) are strictly linked to each other in a highly non-trivial way, and that the evaluation of the non-Markovianity degree of the system dynamics

cannot be simply given by single (tomographic) measurement processes at the time instants t_k's. As a matter of fact, from a sequence of quantum measurements one can have access to the stochastic trajectories of the system while it is interacting with the environment, while from a single measurement we can get information on the state of the system only in one time instant. As a result, in such a case the dynamical evolution of the system before such measurement is completely lost.

For all these reasons, in Ref. [3] we compare the multi-time statistics (built over the sequence of outcomes from a sequential measurements procedure) with the conditional stochastic dynamics, given by the set of system trajectories resulting by applying the measurements. We have identified in the transfer tensor (TT) method [4] the way to propagate the state from the reduced dynamics of $\mathbb{S}$ at the time instant t_k, by starting from the initial state $\rho_{\mathbb{S},0}$ and taking into account possible memory effects occurring during the system evolution. The TT method relies on using the so-called transfer tensors $T_{k,j}$, which are defined by the relation

$$\Phi_k = \sum_{j=0}^{k-1} T_{k,j}\Phi_j, \;\; \text{i.e.,} \;\; T_{k,0} = \Phi_k - \sum_{j=1}^{k-1} T_{k,j}\Phi_j \;\; , \tag{1}$$

where $\Phi_k \equiv \Phi(t_k, t_0)$ denotes the completely positive and trace-preserving (CPTP) quantum maps describing the propagation between $\rho_{\mathbb{S},0}$ and $\rho_{\mathbb{S},k}$, i.e., $\rho_{\mathbb{S},k} = \Phi_k[\rho_{\mathbb{S},0}]$. In this way, the state of $\mathbb{S}$ at t_k is propagated according to the equation

$$\rho_{\mathbb{S},k} = \sum_{j=0}^{k-1} T_{k,j}\rho_{\mathbb{S},j} \;\; . \tag{2}$$

As also shown in [5], through appropriate mathematical calculations one can have access to the complete hierarchy of $1-$, $2-$,...,$n-$step TTs, by which the Markovian component of the system's evolution can be separated from the non-Markovian one. In this regard, in [3] we have proved the following theorem:

Theorem 1: The (discrete) dynamics $\{\Phi_k\}_{k=1,\ldots,m}$ is Markovian if all the transfer tensors $T_{k,k-n}$ are equal to 0 for $n \geq 2$.

The previous result links a property of the hierarchy of TTs to the Markovianity of the corresponding dynamics. As a matter of fact, the thesis of the theorem entails the relation

$$\Phi_k = \Gamma_{k,k-1}\Gamma_{k-1,k-2}...\Gamma_{j+1,j}\Phi_j \;\; , \tag{3}$$

where $\Gamma_{j+1,j}$, with $j = 1, \ldots, k$, denotes the 1-step conditional operators associated to the reduced dynamics of $\mathbb{S}$. Eq.(3) in turn implies CP-divisibility since the map $\mathcal{E}_{k,j} \equiv \Gamma_{k,k-1}\Gamma_{k-1,k-2}...\Gamma_{j+1,j}$ is CPTP by the definition of the 1-step conditional operators $\Gamma_{j+1,j}$. Thus, if the one-step TTs are the only non-zero TTs, then the dynamical maps can be obtained by only using the 1-step conditional operators. System-environment correlations, despite being present as a consequence of the interaction term within the unitary operators, will not affect the reduced dynamics of the open system, so that at any time t_{k-n} the actual global state can be effectively replaced by the product state $\rho_{\mathbb{S},k-n} \otimes \rho_{\mathbb{E},k-n}$. Such a property is in general stronger than the simple CP-divisibility of the dynamics, and in fact the latter does not imply that $T_{k,k-n} = 0$ for $n \geq 2$, as follows from the analysis of [6].

Now, let us assume that the open quantum system $\mathbb{S}$ is monitored at the time instants t_k, $k = 1, \ldots, m$. In particular, we take a sequence of quantum measurements locally performed on $\mathbb{S}$ according to the observables $\mathcal{O}_k \equiv F_{\theta_k} \otimes I_{\mathbb{E}}$, where $\{\theta_k\}$ is the set of the possible measurement outcomes while $\{F_\theta\}$ denotes the set of Hermitian positive semi-definite measurement operators. From a dynamical perspective, a measurement of the open system affects not only its current state, but also its future evolution as a consequence of the change in the correlations between the system and the environment due to the measurement itself [2]. The basic notion of dynamics of the open system becomes more subtle, since it cannot be clearly separated from the results of the sequential measurements. For this reason, in [3] the concept of *conditional dynamics* is introduced. The term conditional dynamics means that the system admits a different dynamics for each sequence of measurement outcomes. Explicitly, the conditional dynamics of the system (for fixed global evolution $\mathcal{U}_{t_s:t_k}$ and initial environmental state $\rho_{\mathbb{E},0}$) is given by the following CTPT map

$$\widetilde{\Phi}_k^{\underline{\theta},\underline{t}}[\rho_{\mathbb{S},0}] \equiv \mathrm{Tr}_{\mathbb{E}}\left[\mathcal{U}_{t_{k-1}:t_k}(\mathcal{P}_{\theta_{k-1}} \otimes \mathbb{1}_{\mathbb{E}}) \cdots (\mathcal{P}_{\theta_1} \otimes \mathbb{1}_{\mathbb{E}})\mathcal{U}_{t_0:t_1}[\rho_{\mathbb{S},0} \otimes \rho_{\mathbb{E},0}]\right] \;\; , \tag{4}$$

depending on the time instants $\underline{t} \equiv (t_1, \ldots, t_k)$ as well as on the measurement outcomes $\underline{\theta} \equiv (\theta_1, \ldots, \theta_{k-1})$. In other terms, $\widetilde{\Phi}_k^{\underline{\theta},\underline{t}}$ has to be understood as a stochastic map, so that we could effectively define different trajectories in the

set of CPTP maps, each of them associated with a different sequence of measurement outcomes. The joint probability distributions to get the measurement outcomes $\theta_1, \theta_2, \ldots, \theta_k$ at time instants $t_1, t_2, \ldots, t_k$ is directly linked to the stochastic map $\widetilde{\Phi}_k^{\underline{\theta},\underline{t}}$ by the following relation:

$$q_k \equiv \text{Prob}(\theta_k, t_k; \ldots; \theta_1, t_1) = \text{Tr}[\mathcal{P}_{\theta_k} \widetilde{\Phi}_k^{\underline{\theta},\underline{t}}[\rho_{\mathbb{S},0}]] \tag{5}$$

that defines the multi-time statistics associated to sequential measurements at different times. Here, it is worth noting that a notion of Markovianity can be associated with them [6, 7] by virtue of the quantum regression theorem [8, 9]. In order to characterize the stochastic dynamics induced by different sequences of outcomes, in [3] we introduce a stochastic version of the TT method, denoted as $\widetilde{T}_{k,j}^{\underline{\theta},\underline{t}}$, $k, j = 1, \ldots, m$, and explicitly depending on the instants and outcomes of the repeated measurements. One can prove that also the set of stochastic transfer tensors admits a hierarchic structure, very similar to that of Eq. (1), based on conditional operators. The main difference, indeed, is that now the conditional operators act on the reduced dynamics of $\mathbb{S}$ at each t_k, after that a quantum measurement has been performed on the system, so that the conditional operators will depend on the resulting post-measurement environmental state. Such hierarchical structure has allowed us to bring forward the connection between TTs and Markovianity to the stochastic level describing sequential measurements. In particular, we have the following [3]:

Theorem 2: For any sequence of outcomes, the stochastic dynamics $\{\widetilde{\Phi}_k^{\underline{\theta},\underline{t}}\}_{k=1,\ldots,m}$ is Markovian if all the stochastic TTs $\widetilde{T}_{k,k-n}^{\underline{\theta},\underline{t}}$ are equal to 0 for $n \geq 2$.

As proved in [3], Theorem 2 is satisfied whenever the global state after the measurements is a product state. This means that in these situations the stochastic dynamics $\widetilde{\Phi}_k$ will be automatically Markovian, simply due to the kind of measurement employed, in this way clearly showing the difference between the notion of Markovianity we associated to the stochastic maps and that referred to the unconditional, deterministic dynamics. Let us note that, in general, the Markovianity of the stochastic dynamics is also different to the notion associated with the multi-time statistics, i.e., the validity of the quantum regression theorem. The latter is in fact recovered only if the dependence of the post-measurement environmental state $\widetilde{\rho}_{\mathbb{E}}$ on the sequence of outcomes can be neglected.

The connection between the stochastic version of the transfer tensor method, introduced by UNIFI, and the non-Markovianity degree of the quantum trajectory of $\mathbb{S}$ originated by its monitoring is still under investigation. In this regard, we are planning to introduce a proper notion of memory induced by the presence of the external observer, which has to be distinguished by the notion of memory induced by system-environment interactions, leading to standard quantum non-Markovianity.

II. Non-Markovian sensing by deep learning and experimental test with optical platforms (UNIFI, INRIM)

For this task here we discuss theoretical and experimental methods to extract information on specific features of the environment/sample from non-Markovianity phenomena occuring on the quantum system used as a probe. In this respect one possibility is to extract such information from the so-called survival probability of finding the probe in its initial state, for instance by also exploiting deep learning techniques. The theory was developed by UNIFI and is currently tested experimentally on a single-photon platform at INRIM.

In particular, we assume that the interaction with the probe does not modify the features of the environment that we aim to infer. Indeed, the only effects due to probe-environment interactions are enclosed within the dynamics of the probe. As in the noise spectroscopy context [10], the evolution of the probe is still governed by a Hamiltonian dynamics that, however, is affected by a fluctuating (noise) field. The latter is a stochastic process, whose autocorrelation function (or power spectral density, in the frequency domain) brings information on the environment giving rise to the stochastic field. Thus, the inference/reconstruction of the noise power spectral density is the final goal of any noise sensing procedure [11–13]. As it has been mainly shown in [14], the samples composing the stochastic noise field in a given time interval $[0, T]$ can be related among them by means of one or more correlation parameters, which entail a coloured noise spectrum. The latter leads to temporal sequences of non-statistically independent noise samples, and thus to memory effects in the probe dynamics.

These phenomena have been theoretically studied by UNIFI during the first year of PATHOS and are currently under investigation on the experimental optical platform at INRIM, introduced in Ref. [15] where an active protection protocol of single photon quantum states has been recently tested. In particular, in [15] the authors propose a method for the measurement of the expectation value of a physical variable on a single particle in a single run of the experiment. This result is in agreement with the theoretical predictions in Refs. [16, 17] whereby in the quantum Zeno

regime (given by consecutive dynamical evolutions separated by frequent projective observations) the outcome from a single measurement, defined by the *most probable value* of the probability to detect a specific feature of the system, is practically overlapped with the expectation value of the measured observable. At the physical level, in the optical platform designed in [15] heralded single photons are produced by type-I parametric down-conversion and prepared in a given initial (product) state

$$|\psi_{\rm in}\rangle = |\psi_\theta\rangle \otimes |\psi_x\rangle, \tag{6}$$

where $|\psi_\theta\rangle = \cos\theta|H\rangle + \sin\theta|V\rangle$ takes into account the polarization degrees of freedom of the photon while $|\psi_x\rangle$ concerns the corresponding spatial degrees of freedom. Afterwards, the photon passes through a birefringent material, whose action is to shift the photons in the transverse direction according to its polarization. In the experiment the number N of birefringent materials is taken smaller than 10. Then, the protection of the polarization state $|\psi_\theta\rangle$ is realized by inserting a thin-film polarizer after each birefringent unit, with the aim to project the photon onto the same polarization state as the initial state. More formally, the interaction of the photon with the non-linear crystals of the setup can be described by the unitary transformation

$$U = e^{ig\,|H\rangle\langle H|\otimes P}, \tag{7}$$

where P is the momentum conjugated to the photon pointer variable and g denotes the coupling constant between P and the projector $|H\rangle\langle H|$, corresponding to the horizontal polarization of the photon. The protection mechanism is realized by the projector

$$\Pi_\theta = |\psi_\theta\rangle\langle\psi_\theta| \otimes \mathbb{I} \tag{8}$$

that "resets" the polarization of the photon to the value assigned by $|\psi_\theta\rangle$. In absence of any noise source, the final wave-function $|\psi_{\rm out}\rangle$ is given by the repeated interaction of the input photon with the sequence of N pairs (birefringent crystal, polarizing plates). The probability that the single photon survives after N interaction-state protection stages is called *survival probability* and is equal to $\mathcal{P}_N \equiv |\langle\psi_{\rm out}|\psi_{\rm out}\rangle|^2$. If the photon is not lost, then the probability is conserved and $\mathcal{P}_N = 1$. In this regard, the most informative quantity to measure is the probability of finding the photon in a specific position x_0 of a spatial-resolving single-photon detector. Such probability is defined as

$$\mathcal{P}_N(x_0) \equiv |\langle\psi_{\rm out}|\Pi_{x_0}|\psi_{\rm out}\rangle|^2, \tag{9}$$

where $\Pi_{x_0} \equiv \mathbb{I} \otimes |x_0\rangle\langle x_0|$.

However, as any other realistic physical scenario, also this experimental setup is unavoidably affected by noise sources. In particular, the polarization angle θ and the coupling constant g are in general stochastic processes defined by a collection of random variables, sampled each time by a specific probability distribution. Accordingly, this necessarily implies a *non-ideal* Zeno protection scenario [16, 18], so that the final wave-function $|\psi_{\rm out}\rangle$ of the single photon is given by a stochastic sequence of N interactions and protection stages. Thus, also the survival probability $\mathcal{P}_N(x_0)$ (probability to find the photon in a specific position x_0 of the space-resolving detector) is a random variable. Indeed, after each realization, $\mathcal{P}_N(x_0)$ takes a different value, depending on the specific realization of the noise on θ and/or g. As proposed in [19], modeling the effects of noise sources allows one to extract useful information on the noise distribution by measuring the statistics of the survival probability $\mathcal{P}_N(x_0)$. More specifically, let us model the coupling rate g as a stochastic process and introduce the vector $\boldsymbol{g} \equiv [g_1, \ldots, g_N]^T$, collecting the random samples of g along the single realization of the quantum process under investigation. Without loss of generality, we assume that after each sampling process $l = 1, \ldots, N$ the single sample of g can take D different values $g^{(1)}, \ldots, g^{(D)}$, with probabilities $p_{g^{(1)}}, \ldots, p_{g^{(D)}}$. Under the assumption that $\boldsymbol{g}$ is a collection of independent and identically distributed (i.i.d.) random variables sampled from the probability distribution Prob(g), in [19] we are providing analytical results for the inference of the value associated to the probabilities $p_{g^{(1)}}, \ldots, p_{g^{(D)}}$, by making use of the maximum likelihood (ML) method [20] and constrained nonlinear least-squares (NLS) routines [21].

To test the validity of our findings, we have simulated the stochastic scenario with g random, with the aim to understand the behaviour of the survival probability $\mathcal{P}_N(x_0)$ as a function of the noise coefficients. The setup parameters are chosen following Ref. [15]. In particular, the number of interaction-protection stages is $N = 7$, the standard deviation σ of the Gaussian initial photon wave-packet is equal to 0.5 mm and the value of the interaction coupling g is taken within the range $[110, 550]$ μm. Moreover, we have chosen $D = 5$, as it is going to be tested soon in the experiment, and $g^{(k)} = k g_{\rm min}$, with $k = 1, \ldots, 5$ and $g_{\rm min} = 110$ μm. The dynamics of the single photon is along a trajectory of product states between the polarization and space photon degrees of freedom, by starting from $\rho_{\rm in} \equiv |\psi\rangle\langle\psi| \otimes |f_{\rm x}\rangle\langle f_{\rm x}|$ where $|\psi\rangle = (|H\rangle + |V\rangle)/\sqrt{2}$ and x is sampled within the interval $g_{\rm min}[1, d]$ with step $g_{\rm min}$. Here,

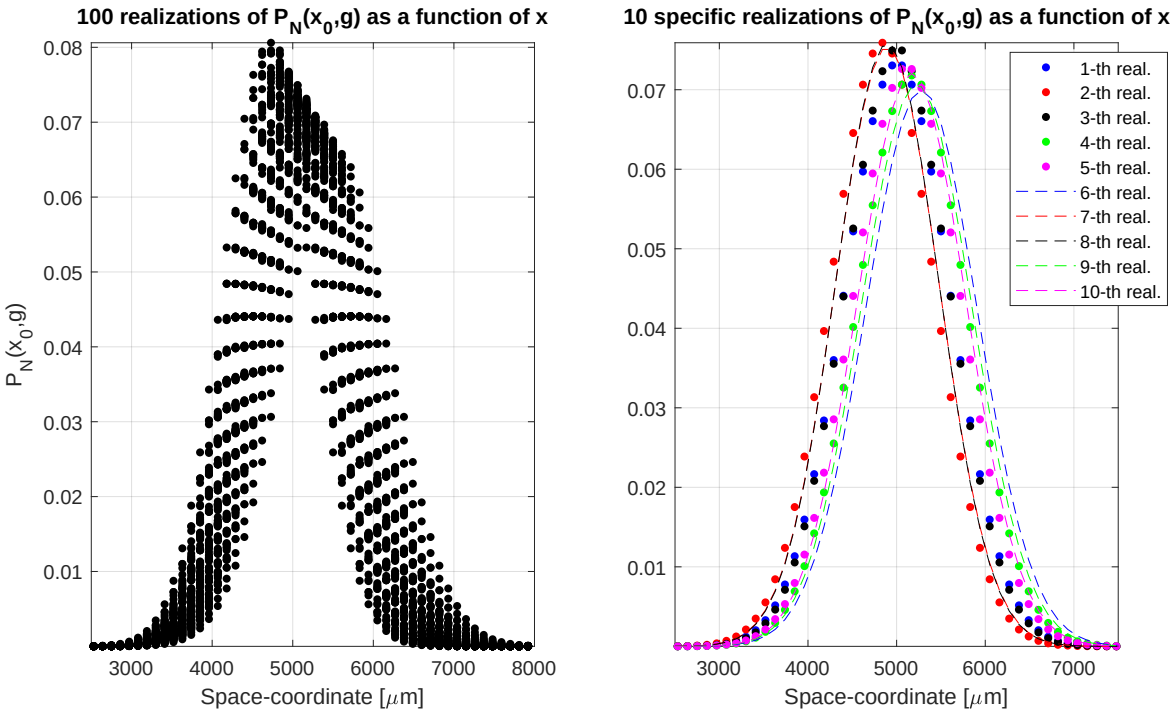

Figure 1: Realizations of the survival probability $\mathcal{P}_N(x_0)$ as a function of the space-coordinate x, with $N = 7$, $D = 5$, $\sigma = 0.5\ mm$, $p_{g^{(1)}}, \ldots, p_{g^{(5)}} = (0.145, 0.285, 0.145, 0.285, 0.14)$, $g_{\min} = 110\ \mu m$, and $g^{(k)} = k g_{\min}$, $k = 1, \ldots, 5$. At $t = 0$ the Gaussian photon wave-packet is initially centered on $x_{\rm in} = 3960\ \mu m$.

d corresponds to the dimension of the reduced Hilbert space associated to the photon spatial degrees of freedom. In Fig. 1 we show a set of realizations of the survival probability $\mathcal{P}_N(x_0)$ as a function of the space-coordinate x. Note that to obtain them we have chosen a specific value for the probabilities $p_{g^{(1)}}, \ldots, p_{g^{(5)}}$, i.e. (0.145, 0.285, 0.145, 0.285, 0.14). The behaviour of $\mathcal{P}_N(x_0)$ mimics the displacement along x of the photon wave-packet with polarization $|\psi\rangle$, imposed by the N protection stages of the implemented mechanism. From Fig. 1, one can extract information about the range of fluctuation of $\mathcal{P}_N(x_0)$ due to the presence of noise on g, hence as a sensing tool.

Moreover, to test the effectiveness of the proposed noise sensing procedure for the reconstruction of the vector $\boldsymbol{p}_g$ of probabilities $p_{g^{(1)}}, \ldots, p_{g^{(D)}}$, we have applied the method in 50 different experiments by taking $\boldsymbol{p}_g$ as random and choosing the same parameters used in Fig. 1, i.e., $N = 7$, $D = 5$, $\sigma = 0.5\ mm$, $g_{\min} = 110\ \mu m$, $g^{(k)} = k g_{\min}$, $k = 1, \ldots, 5$. As shown in Fig. 2, the performance of the proposed sensing strategy are very promising, since, independently of the values of the probabilities p_g (quantities to be estimated) and a quite limited statistics, the reconstruction fidelity

$$\mathcal{F} \equiv 1 - \frac{1}{D} \sum_{k=1}^{D} \left| p_{g^{(k)}} - \hat{p}_{g^{(k)}} \right| , \tag{10}$$

with $\hat{\boldsymbol{p}}_g$ estimated variable, is in the range $[86, 98]\%$ with an average value around 92.6%.

In case the sequence $\boldsymbol{g}$ is not a collection of i.i.d. random variables, the occurrence of each $g^{(k)}$, $k = 1, \ldots, D$, at the discrete time instants t_l, $l = 1, \ldots, N$, will depend on specific sampling of g in previous time instants. In general, for an arbitrary coloured stochastic field analytical methods allowing for the reconstruction of the noise probability distribution, and eventually correlation parameters, are difficult to be determined. For this reason, and also motivated by the idea to design automatic and non-tomographic procedures for the detection of environment features, we have decided to adopt deep learning techniques and in particular (artificial) recurrent neural networks (RNNs). RNN Methods are today extremely successful for text categorization problems and in general to process (temporal) sequences of data [22]. As a matter of fact, the structure of RNNs allows for instance to take into account complex syntactical and semantic structure in the sentences of documents or correlations in temporal sequences. RNNs exhibit an internal state $\boldsymbol{h}$ that changes during the training of the network and recursively depends on the

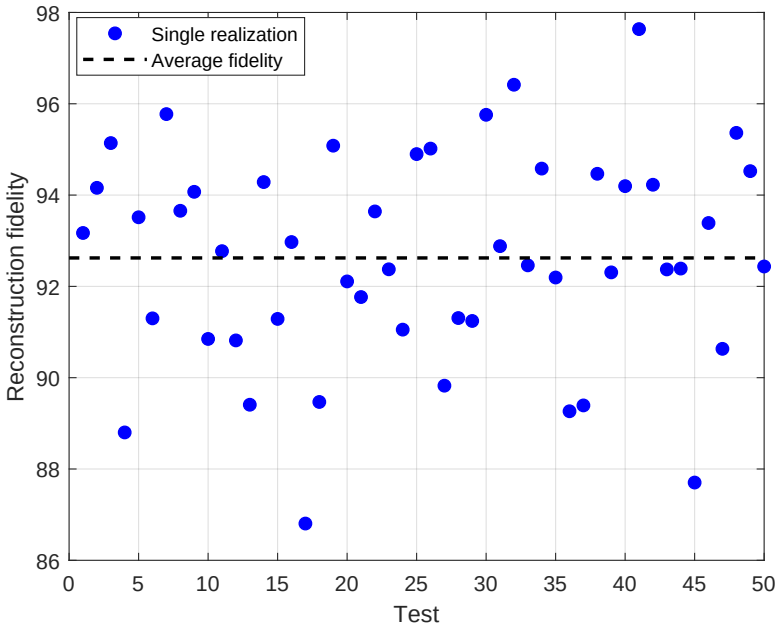

Figure 2: Reconstruction fidelity $\mathcal{F}$ for 50 random different realizations of the probabilities $p_{g^{(1)}}, \ldots, p_{g^{(5)}}$, variables to be inferred. As in Fig. 1, at $t = 0$ the Gaussian photon wave-packet is initially centered on $x_{\text{in}} = 3960\ \mu m$, but L, being the number of protocol realizations for each sequence of p_g, has been chosen equal to 20 in order to test the robustness of the sensing procedure against a quite small sample (i.e. low statistics) of the noise sequences.

state at previous iterations. Precisely, one gets

$$\boldsymbol{h}^{(t)} = f(\boldsymbol{h}^{(t-1)}, \boldsymbol{x}^{(t)}; \boldsymbol{\theta}) \ , \tag{11}$$

where $\boldsymbol{h}$ is the state vector, $\boldsymbol{x}$ is the input vector and $\boldsymbol{\theta}$ are the parameters of the state-function f. The index t indicates the iteration number, which can be interpreted as a discrete time or, more in general, the progressive number of the sequence presented in input. In order to express a compact visualization of a RNN, it is possible to use the graph in fig. 3a where the black box denotes the delay of one iteration (1-step memory cycle). Instead, a pictorial illustration of the unfolding of the graph is shown in fig. 3b.

To detect non-Markovian fluctuating fields, we are hence proposing to adopt a properly designed RNN. The latter, indeed, is expected to allow for the simulation of the inverse dynamics of the already known forward quantum noise prediction model (single photon affected by the noise field under investigation). Such an inversion is prohibitive due to the high complexity of the process. Thus, our basic idea is to collect sufficient data on $\boldsymbol{p}_g \equiv [p_g^{(1)}, \ldots, p_g^{(5)}]^T$ and $\mathcal{P}$ (survival probability) at each time instant t_k, $k = 1, \ldots, 7$ from numerical simulations of the forward prediction model. Then, we will train the model in fig. 4, where each box indicates the implemented RNN, with the aim to attribute the proper value to $\mathcal{P}_k$ and $\boldsymbol{p}_{g_k}$, $k = 1, \ldots, 7$. Once the RNN is trained, the challenge will be to test the model with

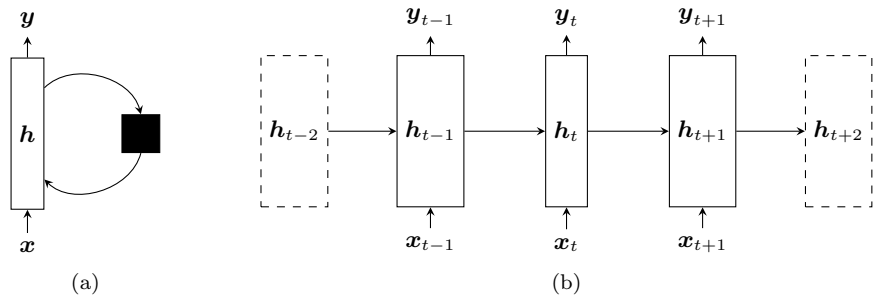

Figure 3: RNNs, folded (a) and unfolded (b) models.

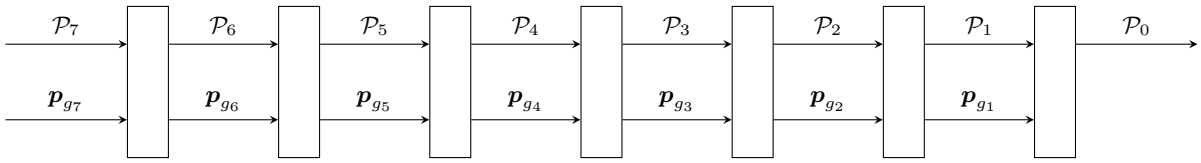

Figure 4: RNN for the sensing of (non-)Markovian fluctuating fields.

real data from the experiment, where, in principle, the only available information are the survival probabilities $\mathcal{P}_0$, $\mathcal{P}_7$ and $\boldsymbol{p}_{g_7}$. We expect that the realization of such neural network corresponds to design an artificial environment able to reproduce all the memory effects induced by the noise fluctuating field.

Finally, another protocol adapted to a similar photonic setup has been theoretically designed from our consortium for the investigation of quantum Zeno and anti-Zeno effects for photon depolarization (dephasing). This protocol aims at observing the inhibition (slowdown) or the enhancement (acceleration) of the quasi-exponential non-Markovian decay of the photon polarization state by means of frequent measurements and soon experimentally tested in the context of a wide collaboration involving UNIFI, INRIM and Weizmann as partners of PATHOS.

Experimental details for the photonics setup (INRIM)

To study these sensing protocols, we are realizing a proof-of-principle experiment exploiting single photons. In our setup, a 76 MHz mode-locked laser at 796 nm is doubled in frequency and injected into a BBO crystal, producing parametric down-conversion (PDC). For photon pair produced, the idler photon at 920 nm heralds the presence of the corresponding signal photon at 702 nm. The signal photon, collimated in a Gaussian mode, is sent through a sequence of K steps (with $1 < K < 7$), each composed of a pair of properly cut birefringent crystals and a polarizer. The first crystal of the pair (slightly) separates the horizontal and vertical components of the polarization, while the second one is used to compensate the temporal and phase walk-off induced. The different coupling strengths g are obtained by using birefringent crystal pairs of different thickness. After the K steps, the photons are fiber coupled and sent to a silicon single-photon avalanche diode, measuring this way the losses induced in the whole interaction process.

III. Sensing resolution in non-Markovian noise spectroscopy via optimally designed filter functions (UNIFI)

Another important open problem we have addressed is whether, with a fixed amount of resources, the reconstruction fidelity of specific features of the sample under investigation, as for example the power spectral density associated to the sample correlation functions, is larger or smaller when the open dynamics of the probe is Markovian or non-Markovian. In other words, we are investigating if one has to store and use more resources to detect sample features involving non-Markovian behaviours in the probe dynamics with respect to Markovian ones, or vice versa.

Numerical simulations in the noise spectroscopy context have shown that the reconstruction fidelity of the power spectral density $S(\omega)$ (defined in the frequency domain) of an external noise fluctuation field affecting a properly chosen quantum system used as a probe is as large as the overlap between $S(\omega)$ and the Fourier transform of the control signals (commonly known as *filter functions*) used to manipulate the probe and to allow for long-time coherence [12, 23]. Thus, by following this simple consideration, we can deduce that for any choice of filter functions (with the only requirement is its physical feasibility) the worst case is given by a *constant* power spectral density $S(\omega)$ acting over all the frequency domain, namely a white noise spectrum. It is well-known that a white fluctuating noise source affecting a quantum system entails a Markovian dynamics of the system itself. Therefore, we expect that with a fixed amount of resources the detection of one or more features of the sample is facilitated if the interaction between the sample and the probe induces non-Markovianity in the probe dynamics. One could thus conjecture a dynamical regime in which one can successfully perform *non-Markovian noise-assisted quantum sensing*. This will be further investigated during PATHOS.

IV. Non-Markovian interacting NV probes (HUJI, Weizmann, UNIFI)

Polarization of nuclear spin baths are at the heart of magnetic resonance imaging (MRI) and nuclear magnetic resonance (NMR). Polarizing a spin bath is the key to enhance the sensitivity of these tools, leading to new analytical capabilities and improved medical diagnostics. During the first year of PATHOS, we have studied the adverse role of quantum correlations (entanglement) in the spin bath that can impede its cooling in many realistic scenarios. We have proposed to remove this impediment by modified cooling schemes, incorporating probe-induced dis-entanglement or, equivalently, alternating non-commuting probe-bath interactions to suppress the buildup of quantum correlations in the bath. This is expected to have implications for sensing applications and will be further texted in PATHOS experimental platforms.

Advanced control of interacting spin systems (HUJI)

Spin Hamiltonian engineering in solid-state systems plays a key role in a variety of applications ranging from quantum information processing and quantum simulations to novel studies of many-body physics. By analyzing the irreducible form of a general two-body spin-1/2 Hamiltonian, we identified all interchangeable interaction terms using rotation pulses. Based on this identification, we derived novel pulse sequences, defined by an icosahedral symmetry group, providing the most general achievable manipulation of interaction terms. We demonstrated that, compared to conventional Clifford rotations (Fig. 5), these sequences offer advantages for creating Zeeman terms essential for magnetic sensing, and could be utilized to generate new interaction forms. The exact series of pulses required to generate desired interaction terms can be determined from a linear programming algorithm (Fig. 6). For realizing the sequences, we proposed two experimental approaches, involving pulse product decomposition, and off-resonant driving. Resulting engineered Hamiltonians could contribute to the understanding of many-body physics, and result in the creation of novel quantum simulators and the generation of highly-entangled states, thereby opening avenues in quantum sensing and information processing.

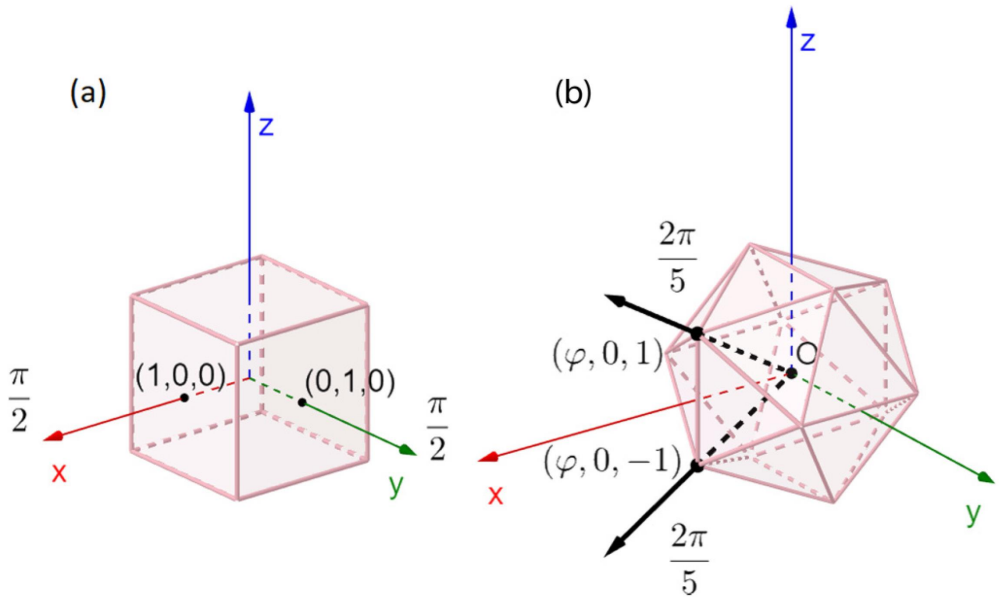

Figure 5: Schematic of the angles and axes of pulses derived from (a) Clifford and (b) icosahedral symmetry groups, with $\phi = (1 + \sqrt{5})/2$ the golden ratio [24].

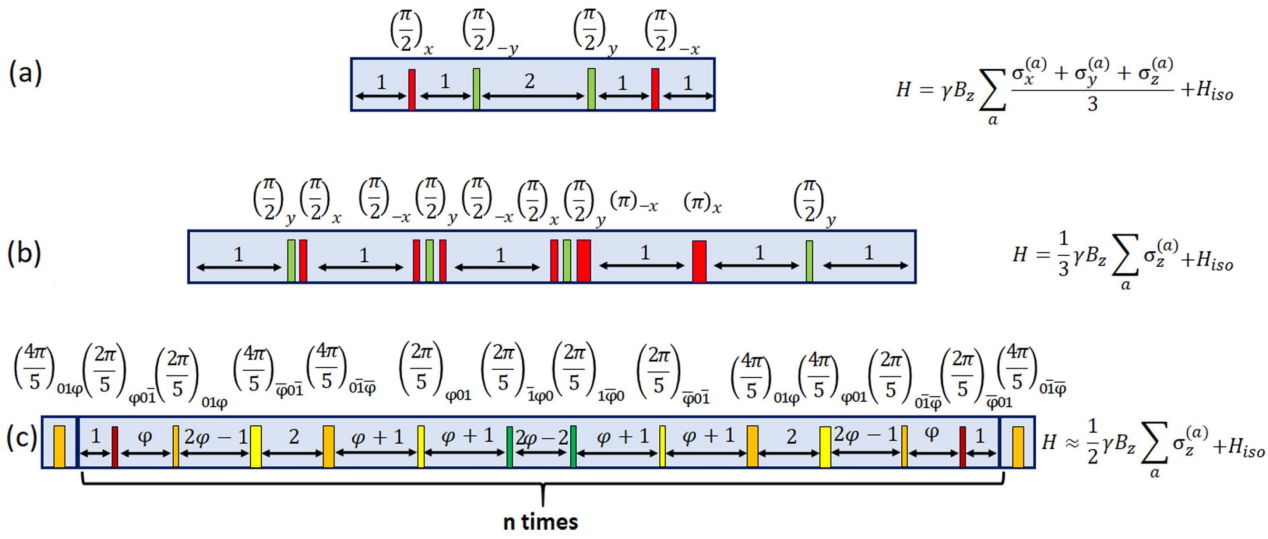

Figure 6: Pulse sequences generating various target Hamiltonians (right column) from the initial NV-NV interaction Hamiltonian: (a) Averaged out dipolar interactions by utilizing the WAHUHA sequence. (b), (c) Zeeman Hamiltonian essential for magnetic sensing, utilizing pulses taken from the (b) Clifford and (c) icosahedral symmetry groups. The icosahedral sequence results in a stronger Zeeman term. Rotation angles and axes are presented above each schematic, time spacings between pulses are given in arbitrary units [24].

Efficient noise spectroscopy (HUJI)

Spin-bath noise characterization, which is typically performed by multi-pulse control sequences, is essential for understanding most spin dynamics in the solid-state. We theoretically proposed a method for extracting the characteristic parameters of a noise source with a known spectrum, using modified Hahn-echo pulses (Fig. 7). By varying the application time of the pulse, measuring the coherence curves of an addressable spin, and fitting these curves to a theoretical function derived by us, we extracted parameters characterizing the physical nature of the noise. Assuming a Lorentzian noise spectrum, we illustrated this method for extracting the correlation time of a bath of nitrogen paramagnetic impurities in diamond, and its coupling strength to the addressable spin of a nitrogen-vacancy center. First, we demonstrated that fitting conventional Hahn-echo measurements to the explicit coherence function is essential for extracting the correct parameters in the general physical regime, for which common methods relying on the assumption of a slow bath are inaccurate. Second, considering a realistic experimental scenario with a 5% noise floor, we simulated the extraction of these parameters utilizing the asymmetric Hahn-echo scheme (Fig. 7). The scheme is effective for samples having a natural homogeneous coherence time ($T2$) up to two orders of magnitude greater than the inhomogeneous coherence time ($T_2{}^*$). In the presence of realistic technical drifts for which averaging capabilities are limited, we simulated more than a factor of 3 improvement of the extracted parameter uncertainties over conventional Hahn-echo measurements (Fig. 8). Beyond its potential for reducing experiment times by an order-of-magnitude, such single-pulse noise characterization could minimize the effects of long time-scale drifts and accumulating pulse imperfections and numerical errors.

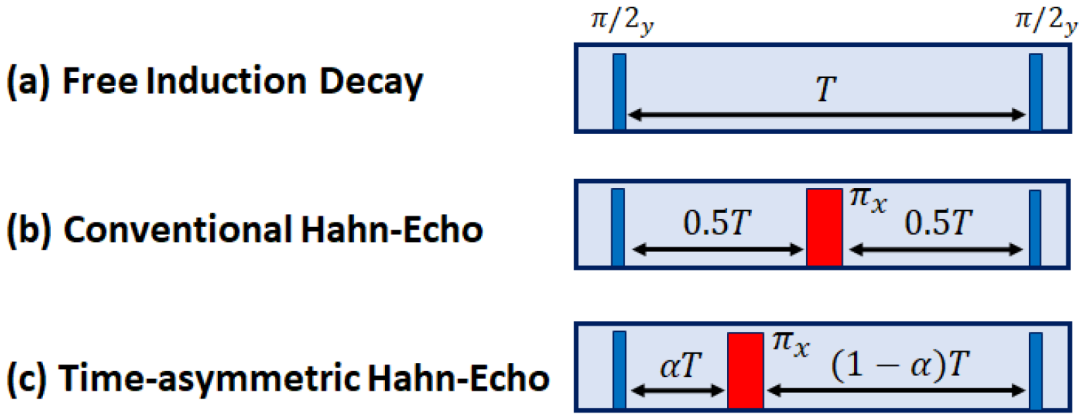

Figure 7: Conventional free-induction decay and Hahn-echo sequences, and the time-asymmetric Hahn-echo sequence [25].

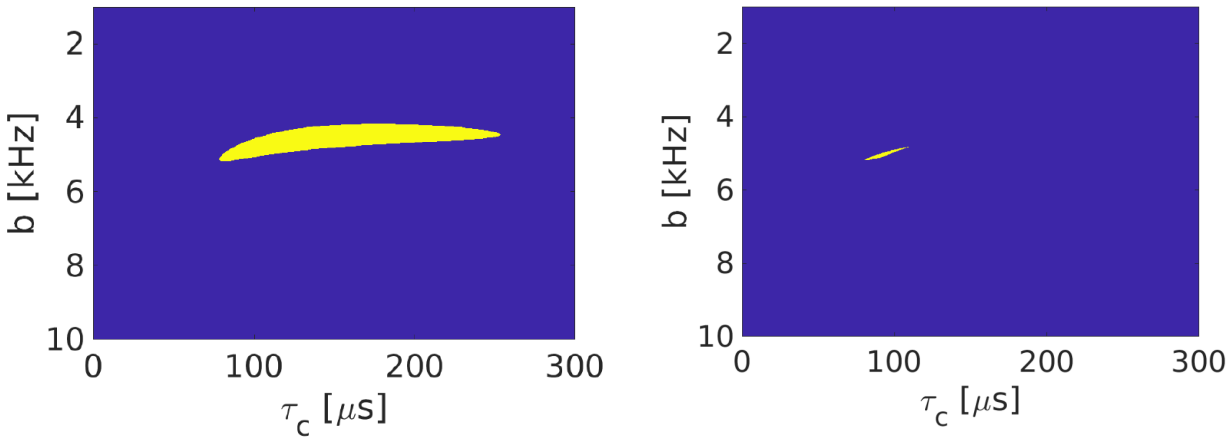

Figure 8: Comparison of the uncertainty in extracted bath parameters (b and (τ_c), for the regular Hahn-echo sequence (left) and the time-asymmetric sequence (right), under the same noise conditions. The asymmetric sequence achieves significantly improved accuracies for a given integration time [25].

[1] A. Rivas, S.F. Huelga, and M.B. Plenio. Quantum non-Markovianity: characterization, quantification and detection. Rep. Prog. Phys. **77**, 094001 (2014).

[2] H.-P. Breuer, E.-M. Laine, J. Piilo, and B. Vacchini. *Colloquium*: Non-Markovian dynamics in open quantum systems. Rev. Mod. Phys. **88**, 021002 (2016).

[3] S. Gherardini, A. Smirne, S. Huelga, and F. Caruso. In preparation (2020).

[4] J. Cerrillo, and J. Cao. Non-Markovian dynamical maps: Numerical processing of open quantum trajectories. Phys. Rev. Lett. **112**, 110401 (2014).

[5] F.A. Pollock, and K. Modi. Tomographically reconstructed master equations for any open quantum dynamics. Quantum **2**, 76 (2018).

[6] L. Li, M.J. W. Hall, H.M. Wiseman. Concepts of quantum non-Markovianity: A hierarchy. Phys. Rep. **759**, 1 (2018).

[7] A. Smirne, D. Egloff, M. Garcia Diaz, M.B. Plenio, and S.F. Huelga. Coherence and non-classicality of quantum Markov processes. Quantum. Sci. Tech. 4, 01LT01 (2019).

[8] C. W. Gardiner and P. Zoller, *Quantum Noise: A Handbook of Markovian and Non-Markovian Quantum Stochastic Methods with Applications to Quantum Optics* (Springer, Berlin, 2004).

[9] G. Guarnieri, A. Smirne, and B. Vacchini. Quantum regression theorem and non-Markovianity of quantum dynamics. Phys. Rev. A **90**, 022110 (2014).

[10] C.L. Degen, F. Reinhard, and P. Cappellaro. Quantum sensing. Rev. Mod. Phys. **89** 035002 (2017).

[11] J. Bylander, S. Gustavsson, F. Yan, F. Yoshihara, K. Harrabi, G. Fitch, D.G. Cory, Y. Nakamura, J.-S. Tsai, and W.D. Oliver. Noise spectroscopy through dynamical decoupling with a superconducting flux qubit. Nat. Phys. **7**, 56570 (2011).

[12] M.M. Müller, S. Gherardini, and F. Caruso. Noise-robust quantum sensing via optimal multi-probe spectroscopy. Sci. Rep. **8**, 14278 (2018).

[13] H.-V. Do, C. Lovecchio, I. Mastroserio, N. Fabbri, F.S. Cataliotti, S. Gherardini, M.M. Müller, N. Dalla Pozza, and F. Caruso. Experimental proof of quantum Zeno-assisted noise sensing. New J. Phys. **21**, 113056 (2019).

[14] M.M. Müller, S. Gherardini, and F. Caruso. Stochastic quantum Zeno-based detection of noise correlations. Sci. Rep. **6**, 38650 (2016).

[15] F. Piacentini, A. Avella, E. Rebufello, R. Lussana, F. Villa, A. Tosi, M. Gramegna, G. Brida, E. Cohen, L. Vaidman, I.P. Degiovanni, and M. Genovese. Determining the quantum expectation value by measuring a single photon, Nat. Phys. **13**, 1191 (2017).

[16] S. Gherardini, S. Gupta, F.S. Cataliotti, A. Smerzi, F. Caruso, S. Ruffo. Stochastic Quantum Zeno by Large Deviation Theory, New J. Phys. **18(1)**, 013048 (2016).

[17] S. Gherardini, C. Lovecchio, M.M. Mueller, P. Lombardi, F. Caruso, F.S. Cataliotti. Ergodicity in randomly perturbed quantum systems, Quantum Sci. Technol. **2(1)**, 015007 (2017).

[18] M.M. Mueller, S. Gherardini, and F. Caruso. Quantum Zeno dynamics through stochastic protocols, Annalen der Physik **529(9)**, 1600206 (2017).

[19] F. Caruso et al., Stochastic quantum Zeno-based sensing on a quantum optical platform. In preparation (2020).

[20] T.A. Severini. Likelihood Methods in Statistics (New York: Oxford University Press, 2000).

[21] G.A.F. Seber, and C.J. Wild. Nonlinear Regression (John Wiley & Sons, Inc., New York, 1989).

[22] I. Goodfellow, Y. Bengio, and A. Courville. *Deep Learning* (MIT Press, 2016).

[23] N. Dalla Pozza, S. Gherardini, M.M. Müller, and F. Caruso, Role of the filter functions in noise spectroscopy. Eprint arXiv:1911.10598 (2019), accepted for publication in the International Journal of Quantum Information.

[24] K.I. O. BenAttar et. al., Phys. Rev. Research 2, 013061 (2020).

[25] D. Farfurnik and N. Bar-Gill, accepted in PRB (2020).